Human Brain Mapping

WILEY

REVIEW ARTICLE OPEN ACCESS

Network-Level Convergence of Adiposity-Related Gray Matter Alterations: A Coordinate-Based Connectome Mapping Meta-Analysis With Imaging Transcriptomics

Yingxian Li | Mingnan Lin | Gengbiao Zhang | Hongyi Zheng | Wenbin Zheng

Department of Medical Imaging, The Second Affiliated Hospital of Shantou University Medical College, Shantou, Guangdong Province, China

Correspondence: Wenbin Zheng (hwenb@126.com)

Received: 17 February 2026 | **Revised:** 30 April 2026 | **Accepted:** 21 May 2026

Keywords: adiposity | gray matter volume | imaging transcriptomics | obesity | voxel-based morphometry

ABSTRACT

Obesity is commonly associated with atrophy-like gray matter changes, such as lower gray matter volume or density, yet the affected regions reported vary widely across studies. It remains unclear whether these heterogeneous loci converge on a reproducible large-scale network, and whether weight-loss–related increases in gray matter map onto the same network or a distinct set of functional systems. We identified loci of adiposity-related gray matter reduction and post-weight-loss increases from 38 published whole-brain voxel-based morphometry studies, including case–control, dimensional adiposity, and longitudinal weight-loss contrasts. Using coordinate-based connectome mapping applied to a large normative resting-state functional connectome, we reconstructed networks associated with adiposity-related structural alterations. We further performed imaging transcriptomic and gene set enrichment analyses to characterize the molecular programs associated with the adiposity-related network. Gray matter reductions associated with adiposity converged on a reproducible, distributed large-scale network primarily involving frontoparietal control, cingulo-opercular, default mode, and Visual1 systems. In contrast, GMV/GMD increases following weight loss showed a distinct system-level distribution, with the largest contributions in cingulo-opercular, somatomotor, and dorsal attention systems, and comparatively limited representation in default mode and frontoparietal control networks. Imaging transcriptomic analyses further linked the adiposity-related network to coordinated gene expression patterns, and gene set enrichment analyses highlighted pathways related to mitochondrial energy metabolism, synaptic signaling, ion transport, and cellular protein homeostasis. Adiposity-related gray matter alterations converge on a reproducible large-scale network, but the system-level pattern differs across categorical obesity, dimensional adiposity, and GMV/GMD increases following weight loss. Weight-loss–related gray matter increases are not a simple mirror reversal of the cross-sectional network, and imaging transcriptomic analyses implicate coordinated molecular programs related to mitochondrial energetics, synaptic signaling, ion transport, and protein homeostasis.

1 | Introduction

Accumulating evidence suggests that obesity and excess adiposity are associated with lower gray matter volume or density, and that these structural brain alterations may contribute to accelerated cognitive decline and increased risk of mild cognitive impairment and dementia, even after accounting for conventional vascular risk factors (Tang et al. 2021; Qu et al. 2020; Fang et al. 2026; Livingston et al. 2024). Several interacting mechanisms may link excess adiposity to gray matter injury.

Yingxian Li and Mingnan Lin contributed equally to this work.

Key Points

- Cross-sectional adiposity-related GMV/GMD reductions converge on a reproducible large-scale network, mainly involving frontoparietal control, cingulo-opercular, default mode, and Visual1 systems.
- Weight-loss–related GMV/GMD increases show a distinct network distribution, with greater involvement of cingulo-opercular, somatomotor, and dorsal attention systems rather than a simple mirror reversal of the cross-sectional pattern.
- Imaging transcriptomic analyses link the adiposity-associated network to molecular programs related to mitochondrial energetics, synaptic signaling, ion transport, and protein homeostasis.

Adiposity-related insulin resistance may disrupt neuronal insulin signaling, a process essential for synaptic maintenance, dendritic plasticity, and cerebral glucose metabolism, thereby increasing vulnerability in metabolically demanding brain regions (Arnold et al. 2018; Kullmann et al. 2016). In parallel, chronic low-grade inflammation driven by adipose-derived cytokines and adipokines may compromise blood–brain barrier integrity, activate microglia, and promote neuroinflammatory cascades that contribute to regionally selective neuronal injury (Miller and Spencer 2014; O'brien et al. 2017). These metabolic and inflammatory insults may be especially consequential in higher-order association regions, including regions within the default mode, frontoparietal control, and salience networks, which are characterized by high metabolic demand and dense synaptic connectivity (Vaishnavi et al. 2010; Crossley et al. 2014; Morys et al. 2024). Because these same systems are also implicated in cognitive aging and neurodegenerative disease, defining the network-level topography of adiposity-related gray matter alterations may help clarify cognitive risk, identify targets for monitoring treatment effects, and determine whether such changes reflect a modifiable component of brain aging (Rubino et al. 2025; Buckner et al. 2008; Honea et al. 2016; Li et al. 2023; The Lancet Diabetes Endocrinology 2025; Maynard 2025).

VBM studies have reported lower gray matter volume or density in overweight and obesity, particularly in prefrontal, insular, temporal, and cingulate regions (García-García et al. 2019; Li et al. 2022; Pannacciulli et al. 2006; Brooks et al. 2013; Jauch-Chara et al. 2015). Yet these findings remain spatially heterogeneous across studies, making it unclear whether they converge on common functional brain networks (Li et al. 2022).

Importantly, adiposity-related structural alterations may be at least partly reversible. Longitudinal VBM studies after bariatric surgery have reported gray matter increases following substantial weight loss, with some effects persisting for up to 24 months and covarying with metabolic or inflammatory improvement (Rullmann et al. 2018). This question is clinically important because it may help identify which brain changes are potentially modifiable with treatment, and whether post-weight-loss remodeling reflects true recovery within the same vulnerable systems or a distinct pattern of structural reorganization.

Despite this progress, two key gaps remain. Conventional coordinate-based meta-analyses identify convergent peaks but provide limited insight into whether heterogeneous adiposity-related loci converge on coherent large-scale networks. This issue is especially relevant given the spatial heterogeneity and phenotype dependence of adiposity-related gray matter findings (Liu et al. 2025). Normative connectome-based mapping addresses this limitation by projecting focal loci onto intrinsic connectivity networks derived from large resting-state datasets (Fornito et al. 2015; Fox 2018; Stubbs et al. 2023). Coordinate network mapping, in particular, offers a framework for revealing network-level convergence not captured by standard ALE-style summaries (Fox 2018; Lefort-Besnard et al. 2025; Peraza et al. 2025; Steele et al. 2025).

A further gap concerns biological interpretation. It remains unclear whether the spatial topology of adiposity-related gray matter vulnerability, as expressed across large-scale functional systems, is constrained by specific molecular architectures. Imaging transcriptomics provides a principled framework for linking macroscale neuroimaging patterns to regional gene expression gradients derived from the Allen Human Brain Atlas, thereby enabling pathway-level interpretation of network organization (Arnatkeviciute et al. 2023).

Here, we combined connectome-based mapping with imaging transcriptomics using published whole-brain VBM evidence available through December 1, 2025, to (i) derive networks associated with adiposity-related gray matter reduction and post-weight-loss increases, (ii) situate these networks within canonical functional systems, and (iii) identify gene expression programs that may constrain their spatial organization. A schematic overview of the study workflow is shown in Figure 1.

2 | Methods

2.1 | Literature Search and Eligibility Criteria

We conducted a systematic literature search of PubMed, Web of Science, and Embase for studies published up to December 1, 2025, using combinations of keywords related to adiposity (e.g., body mass index, waist circumference, body fat percentage), gray matter structure, and voxel-based morphometry (Figure S1). Only peer-reviewed studies were considered. Eligible studies were required to report whole-brain voxel-wise analyses of gray matter volume or density (GMV/GMD) in association with primary adiposity measures and to provide peak coordinates in standard stereotactic space (MNI or Talairach). To focus on adiposity-related structural associations, we included only studies in which the primary statistical models examined either categorical or continuous adiposity phenotypes while controlling for basic demographic and anatomical covariates. Three types of contrasts were eligible for inclusion: (i) case–control comparisons between individuals with obesity and individuals with normal weight; (ii) dimensional associations between GMV/GMD and continuous adiposity measures (e.g., body mass index, waist circumference, or body fat percentage); and (iii) longitudinal changes in GMV/GMD following weight-loss interventions.

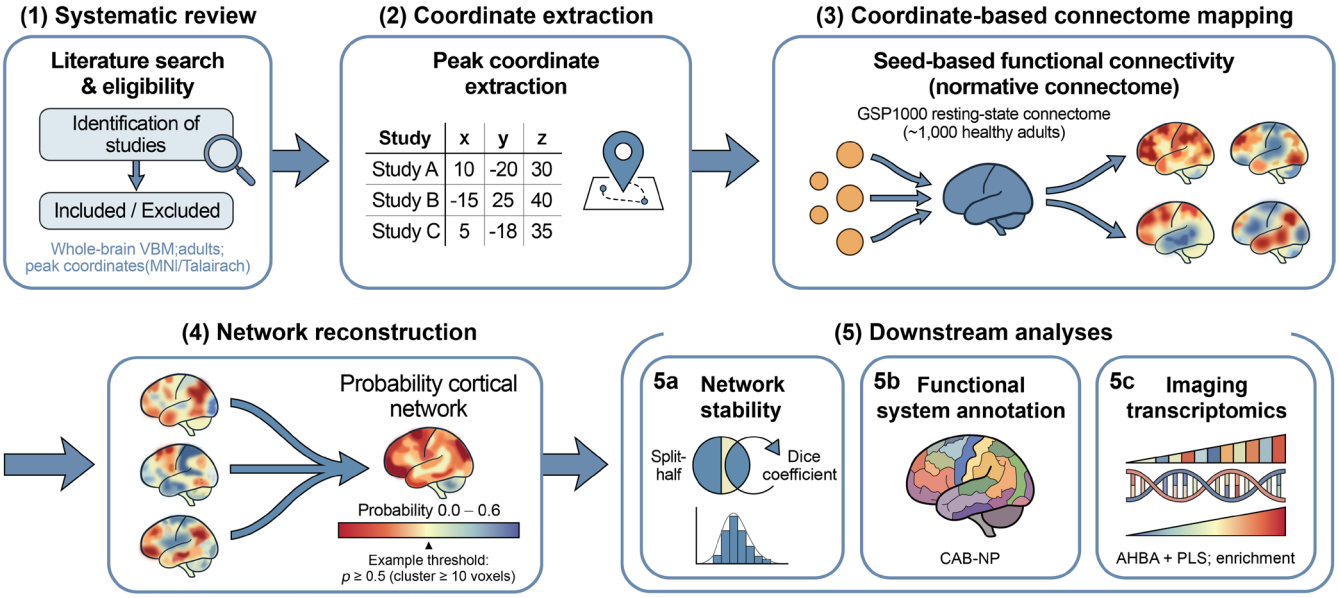

FIGURE 1 | Study overview and analysis workflow. The figure schematically illustrates the analytic pipeline used in this study: (1) systematic literature review and study selection of whole-brain VBM studies; (2) extraction of peak coordinates associated with adiposity-related or weight-loss–related gray matter volume/density (GMV/GMD) alterations; (3) coordinate-based connectome mapping using each coordinate as a seed in a large normative resting-state functional connectome (~1000 healthy adults); (4) aggregation of seed-based connectivity maps across studies to reconstruct probability-based networks; and (5) downstream analyses, including (5a) network stability assessment (split-half resampling), (5b) functional system annotation (CAB-NP), and (5c) imaging transcriptomics linking network topology to regional gene expression from the Allen Human Brain Atlas. The figure is a schematic workflow illustration for visualization purposes.

Detailed inclusion and exclusion criteria are provided in the Supplementary Methods. Based on these criteria, we identified a total of 38 eligible studies, yielding 46 contrasts in total, including 13 case–control contrasts, 21 dimensional adiposity analyses, and 12 longitudinal weight-loss contrasts, with some studies contributing more than one contrast type. Study characteristics are summarized in Supplementary Table S1 (Honea et al. 2016; Pannacciulli et al. 2006; Brooks et al. 2013; Jauch-Chara et al. 2015; Rullmann et al. 2018, 2019; Figley et al. 2016; Hayakawa et al. 2018; He et al. 2015; Hidese et al. 2022; Horstmann et al. 2011; Huang et al. 2019; Karlsson et al. 2013; Kennedy et al. 2016; Kurth et al. 2013; Kharabian Masouleh et al. 2016; Mathar et al. 2016; Michaud et al. 2020; Nouwen et al. 2017; Opel et al. 2017; Prehn et al. 2017, 2020; Shan et al. 2019; Shott et al. 2015; Smucny et al. 2012; Taki et al. 2008; Tuulari et al. 2016; Walther et al. 2010; Wang et al. 2017, 2020; Weise et al. 2013, 2017, 2019; Yao et al. 2016; Yokum et al. 2012; Zhang et al. 2016; Zhou et al. 2025; Janowitz et al. 2015). The methodological quality of included studies was independently assessed using a standardized neuroimaging quality checklist, with full criteria and results reported in Supplementary Methods S1 and Supplementary Table S2.

2.2 | Coordinate-Based Connectome Mapping

To reconstruct networks associated with adiposity-related and weight-loss–related gray matter alterations, we applied a coordinate-based connectome mapping approach. Peak coordinates from eligible contrasts were converted into spherical seed regions in standard MNI space and projected onto a large normative resting-state functional connectome derived from ~1000 healthy adults. Normative functional connectivity data were obtained from the GSP1000 preprocessed connectome of the Brain Genomics Superstruct Project (https://doi.org/10.7910/DVN/ILXJKS) (Holmes et al. 2015). For each seed, whole-brain functional connectivity maps were generated within the normative connectome, thresholded to identify significantly connected regions, and binarized to produce study-level network masks. These masks were combined across studies to derive voxelwise probability-based networks. Because there is no universally accepted overlap threshold for coordinate–/network-mapping–based reconstruction, we used prespecified operational criteria to define the primary network mask for downstream analyses. Specifically, voxels present in at least 50% of study-level maps were retained, and clusters smaller than 10 contiguous voxels were removed to reduce isolated fragments and improve interpretability. Recent network-localization studies have used similar group-level overlap thresholds, typically in the range of 50%–60%, supporting the use of such thresholds as empirical reconstruction parameters rather than fixed standards (An et al. 2026; She et al. 2026; Ma et al. 2026; Liu et al. 2026). Robustness across adjacent convergence thresholds was evaluated in sensitivity analyses (Figure S2). Full details of connectome construction, statistical thresholding, and sensitivity analyses are provided in the Supplementary Methods S2.

2.3 | Network Stability and Spatial Specificity

To assess the robustness of the adiposity-associated networks, we evaluated their spatial stability using a split-half resampling procedure. In each iteration, study-level network masks

were randomly divided into two halves, independently combined to generate two networks, and compared using the Dice similarity coefficient. To determine whether the observed spatial overlap exceeded chance expectations, we constructed size-matched random networks within the same brain mask and repeated the split-half procedure to generate a null distribution of Dice coefficients. The stability and spatial specificity of the observed networks were assessed by comparing the empirical Dice values with this null distribution. Full details of the resampling strategy, random network generation, and statistical evaluation are provided in the Supplementary Methods S3.

2.4 | Functional System Annotation

To characterize the large-scale functional organization of the cross-sectional adiposity-associated gray matter networks, we annotated network voxels using a large-scale functional network atlas. Primary analyses were conducted using the Cole–Anticevic Brain Network Parcellation (CAB-NP, 12-network solution, https://github.com/ColeLab/ColeAnticevicNetPartition) (Ji et al. 2019). Network masks were resampled to the CAB-NP atlas space, and all voxels within the cross-sectional adiposity (including obesity status and dimensional) or weight-loss related networks were treated as affected voxels.

For each functional system, we quantified two complementary metrics: (i) the proportion of total affected voxels located within the system, and (ii) within-network vulnerability, defined as the proportion of voxels affected within each network's total volume. These complementary metrics were used to describe the relative involvement of different large-scale networks.

2.5 | Imaging Transcriptomics Analysis

To relate adiposity-associated network patterns to underlying molecular organization, we performed imaging transcriptomic analyses using regional gene expression data from the Allen Human Brain Atlas. Gene expression data were processed and mapped to brain regions using standardized procedures implemented in the abagen toolbox. A continuous imaging phenotype was constructed by averaging seed-based functional connectivity values across all coordinates contributing to the adiposity-associated network. Mean values were extracted for each Brainnetome region in the left hemisphere (Fan et al. 2016).

Regional gene expression profiles were matched to the same left-hemisphere Brainnetome parcellation, and partial least squares (PLS) regression was used to identify gene expression components associated with the spatial distribution of the imaging phenotype. We evaluated the first two PLS components because they capture the principal axes of covariance between regional gene expression and the imaging phenotype and are commonly examined in imaging–transcriptomic studies. Statistical significance of each latent variable was assessed using spatial permutation testing to account for spatial autocorrelation (Cheng et al. 2025). Because PLS1 represented the dominant latent variable, downstream enrichment analyses were restricted to genes with stable positive contributions to PLS1 (bootstrap $Z > 5$). Positive weights indicate that higher regional gene expression is spatially aligned with higher values of the imaging phenotype. Full details of transcriptomic preprocessing, model implementation, and statistical evaluation are provided in the Supplementary Methods S4 and Supporting Information S1.

2.6 | Gene Set Enrichment Analysis

To characterize the biological processes associated with genes linked to the adiposity-associated network, we performed functional and disease enrichment analyses on genes showing high and stable contributions to the dominant PLS component. Gene Ontology (GO) and Kyoto Encyclopedia of Genes and Genomes (KEGG) pathway enrichment analyses were conducted using the DAVID bioinformatics resource (https://davidbioinformatics.nih.gov/). All enrichment analyses and statistical testing were performed directly within the DAVID platform, with correction for multiple comparisons applied using the Bonferroni method. The resulting enrichment tables were exported from the DAVID website and are provided as supplementary Excel files to ensure transparency and reproducibility. Detailed enrichment results, statistical parameters, and gene lists are reported in the Supplementary Methods and Supporting Information S2.

2.7 | Code Availability and Reproducibility

All preprocessing and analyses were performed using custom-written code in Python (version 3.8) and MATLAB (R2024b). The complete analysis code and parameter settings have been registered and will be made publicly available via the Open Science Framework (OSF; Registration DOI: https://doi.org/10.17605/OSF.IO/SPJZD).

3 | Results

3.1 | Adiposity-Associated Gray Matter Networks

Using coordinate-based connectome mapping, we constructed a network associated with adiposity-related reductions in gray matter volume and density (GMV/GMD) by integrating peak coordinates from cross-sectional case–control and dimensional analyses. Study-level network masks were combined to generate a voxel-wise probability map, and a primary adiposity-associated network was defined using a prespecified threshold (voxel-wise probability ≥ 0.5; minimum cluster size ≥ 10 voxels) for subsequent analyses (Figure 2).

Sensitivity analyses indicated that varying the probability threshold altered network extent but did not change the preferential involvement of higher-order association systems, and no additional spatial foci emerged (Figure S2). Based on these findings, all functional system annotation and imaging transcriptomic analyses were conducted using the primary network. Using the same analytic framework, we also constructed networks associated with longitudinal GMV/GMD changes following weight loss, which are reported separately below.

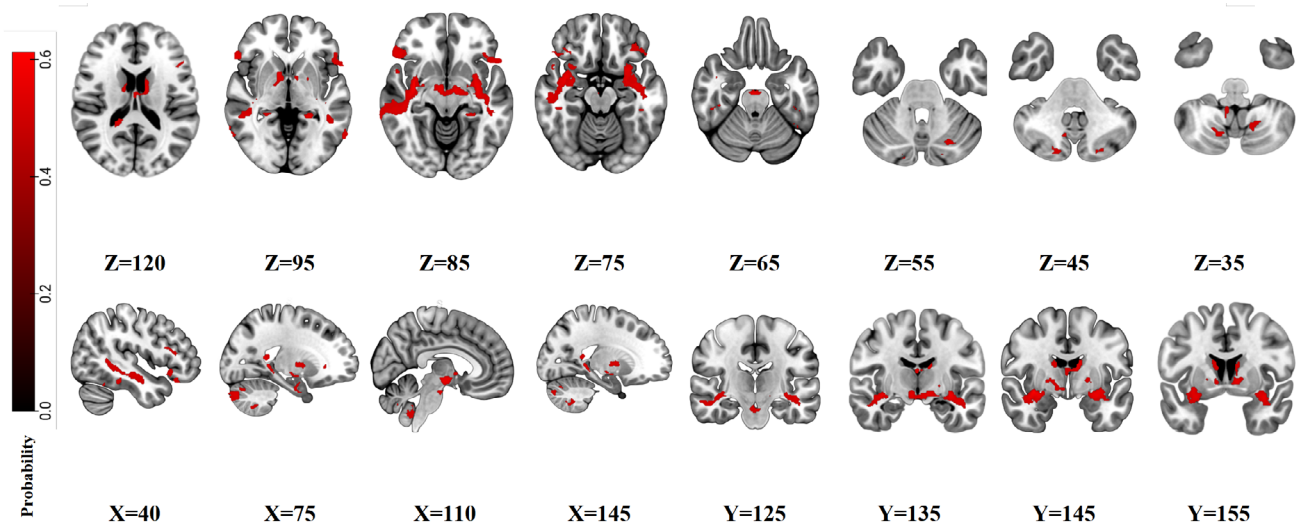

FIGURE 2 | Cross-sectional gray matter network derived from adiposity-related case–control and dimensional analyses. The figure shows a probability-based network derived from coordinate-based connectome mapping of cross-sectional adiposity-related gray matter volume and density (GMV/GMD) reductions. Voxel intensity reflects the probability of network involvement across included contrasts, with darker colors indicating higher spatial consistency. The network was defined using a voxel-wise probability threshold of ≥0.5 and a minimum cluster size of 10 voxels. Representative axial, coronal, and sagittal slices are shown for visualization.

3.2 | Network Stability and Spatial Specificity

We assessed the spatial stability of the cross-sectional adiposity-associated network using split-half resampling, with spatial overlap quantified by the Dice similarity coefficient. Across iterations, the resulting half-sample networks showed consistent spatial overlap, indicating that the identified pattern was reproducible across independent subsets of studies. Spatial specificity was further confirmed by comparison with size-matched random networks constrained to the same brain mask, demonstrating that the observed network convergence exceeded chance expectations (Figure 3).

3.3 | Functional System Distribution of the Cross-Sectional Adiposity-Associated Network

To characterize the functional organization of adiposity-associated gray matter alterations, we projected the cross-sectional adiposity-associated GMV/GMD network onto the CAB-NP large-scale functional atlas (Figure 4A). This network integrated coordinates from cross-sectional case–control and dimensional adiposity analyses and did not include longitudinal weight-loss–related effects.

At the system level, vulnerability associated with adiposity showed a clearly non-uniform distribution across functional networks. The largest proportion of affected voxels was located within higher-order control and association systems, with the frontoparietal control network contributing the greatest share, followed by the cingulo-opercular control network and the default mode network. In contrast, primary sensory and motor systems accounted for relatively small proportions of abnormal voxels.

Within-network analyses showed a partially dissociable pattern. Several association and sensory–association systems exhibited relatively high internal overlap with the adiposity-associated abnormality network despite contributing fewer affected voxels overall. In particular, auditory, posterior multimodal, and language systems showed the highest within-network vulnerability, whereas most other systems showed more modest involvement. Together, these results indicate that cross-sectional adiposity-related GMV/GMD reductions follow a selective system-level organization rather than a diffuse pattern. Exact values are reported in Supplementary Table S3.

3.4 | Phenotypic Heterogeneity: Dissociable System-Level Patterns for Categorical Obesity and Dimensional Adiposity

To examine heterogeneity within the cross-sectional adiposity-related network, we compared system-level distributions derived from categorical case–control contrasts and dimensional adiposity associations. Both analyses were based exclusively on cross-sectional coordinates and excluded longitudinal weight-loss effects. Networks derived from categorical obesity contrasts preferentially involved control and attention-related systems, with the strongest contributions from cingulo-opercular and dorsal attention networks and comparatively smaller contribution from the default mode network (Figure 4B). In contrast, networks derived from dimensional adiposity measures were dominated by default mode and higher-order association systems, with relatively less involvement of salience and attention networks (Figure 4C).

3.5 | System-Level Organization of Weight-Loss–Related GMV/GMD Changes

We next examined the GMV/GMD network associated with weight loss, derived from longitudinal studies comparing

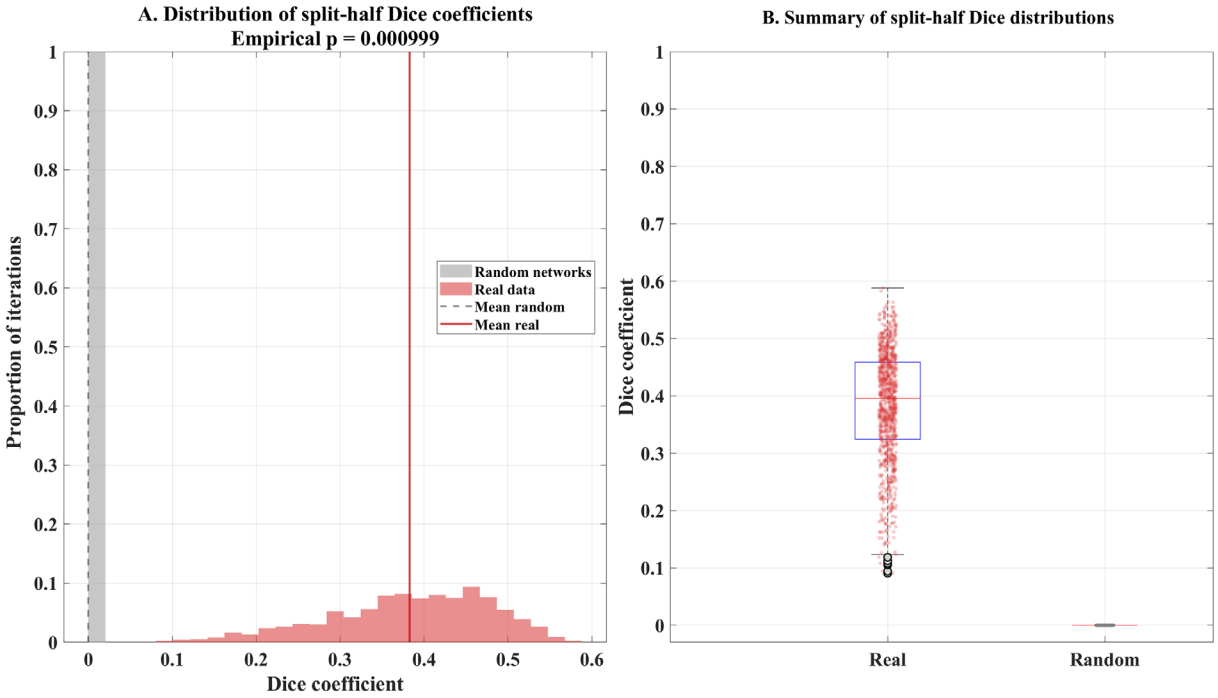

FIGURE 3 | Spatial stability and specificity of the cross-sectional adiposity-associated network. (A) Overlaid probability histograms showing the distributions of split-half Dice coefficients derived from 1000 iterations. The red histogram represents the spatial overlap between independently derived split-half networks using the real data, whereas the gray histogram represents the null distribution generated from size-matched random networks constrained within the same brain mask. The vertical lines indicate the respective mean Dice coefficients (Mean real Dice = 0.38; Mean random Dice = 0.003). The empirical p-value ($p < 0.001$) confirms that the observed spatial convergence significantly exceeds chance expectations. (B) Boxplots with jittered scatter overlays summarizing the variance and data spread of the split-half Dice coefficients for both the real and random network configurations. Each dot represents a single resampling iteration.

brain structure before and after weight-reduction interventions. This network was analyzed separately from the cross-sectional adiposity-related networks. At the system level, the weight-loss–related network showed a distribution distinct from the cross-sectional pattern, with the largest contributions in cingulo-opercular, somatomotor, and dorsal attention systems, and comparatively smaller contributions in frontoparietal and default mode networks (Figure 4D). This distribution argues against a simple mirror reversal of the cross-sectional adiposity-associated network. Within-network analyses showed relatively concentrated involvement of sensorimotor and attention-related systems, supporting preferential engagement of motor, salience, and attentional processes. In contrast, higher-order association networks that were prominent in the cross-sectional analyses showed comparatively limited representation in the weight-loss network.

3.6 | Imaging Transcriptomic Context of Adiposity-Related Network Vulnerability

To characterize the molecular architecture underlying adiposity-related gray matter vulnerability, we related the spatial pattern of the cross-sectional adiposity-related GMV/GMD network to regional gene expression using partial least squares (PLS) regression. PLS analysis identified two significant latent variables. PLS1 explained 28.17% of the variance in the imaging phenotype and PLS2 explained an additional 20.42% (cumulative variance explained by the first two components: 48.59%), with both components reaching significance by spatial permutation testing (PLS1: $r = 0.633$, $p = 0.011$; PLS2: $r = 0.584$, $p = 0.006$; Figure S3). Because PLS1 represented the dominant latent variable, downstream enrichment analyses focused on genes with stable positive weights on PLS1 (bootstrap $Z > 5$), indicating positive spatial association with the imaging phenotype. Functional pathway analyses based on these positively weighted PLS1 genes demonstrated convergent enrichment for molecular processes related to mitochondrial energy metabolism, synaptic structure and signaling, ion transport, and cellular protein homeostasis. These pathways represent core biological programs supporting neuronal energetics, synaptic communication, and excitability regulation in large-scale brain networks.

Disease gene set enrichment further indicated overlap with neurological disorders characterized by impaired energy metabolism and altered neuronal excitability, including epilepsy, primary mitochondrial disorders, and related neurodegenerative disease categories. Although these overlaps do not imply shared disease etiology, they suggest that adiposity-related network vulnerability maps onto transcriptional architectures that are also implicated in conditions marked by energetic failure and excitability imbalance. Together, these findings provide a coherent molecular framework linking systemic metabolic stress to network-level brain vulnerability through conserved pathways governing neuronal energy supply and synaptic function (Figure 5).

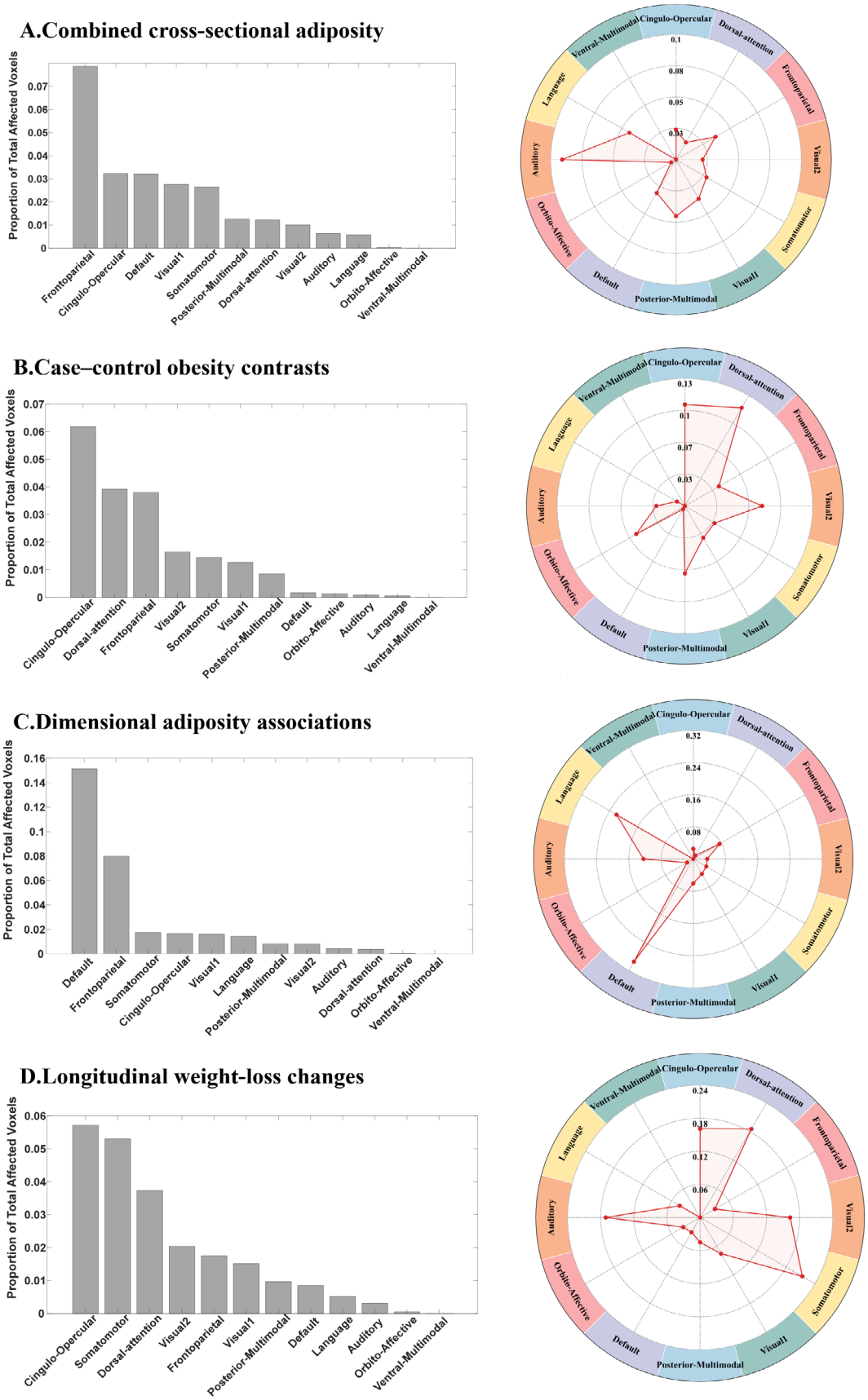

FIGURE 4 | Legend on next page.

FIGURE 4 | System-level organization of adiposity- and weight-loss–related GMV/GMD networks. The figure summarizes system-level distributions of gray matter volume/density (GMV/GMD) networks across four analyses: (A) the cross-sectional adiposity-associated network derived from combined case–control and dimensional analyses; (B) the obesity-related network derived from categorical case–control contrasts; (C) the network derived from dimensional associations with adiposity measures; and (D) the weight-loss-related network derived from longitudinal pre-post intervention studies. For each subfigure, the left panel shows bar plots indicating the proportion of all affected voxels located within each large-scale functional system defined by the CAB-NP atlas. The right panel shows polar plots depicting within-network vulnerability, defined as the proportion of affected voxels within each functional system relative to its total network volume. Together, these complementary metrics illustrate both the relative contribution of each functional system to the overall network and the internal susceptibility of each system to adiposity- or weight-loss-related structural alterations.

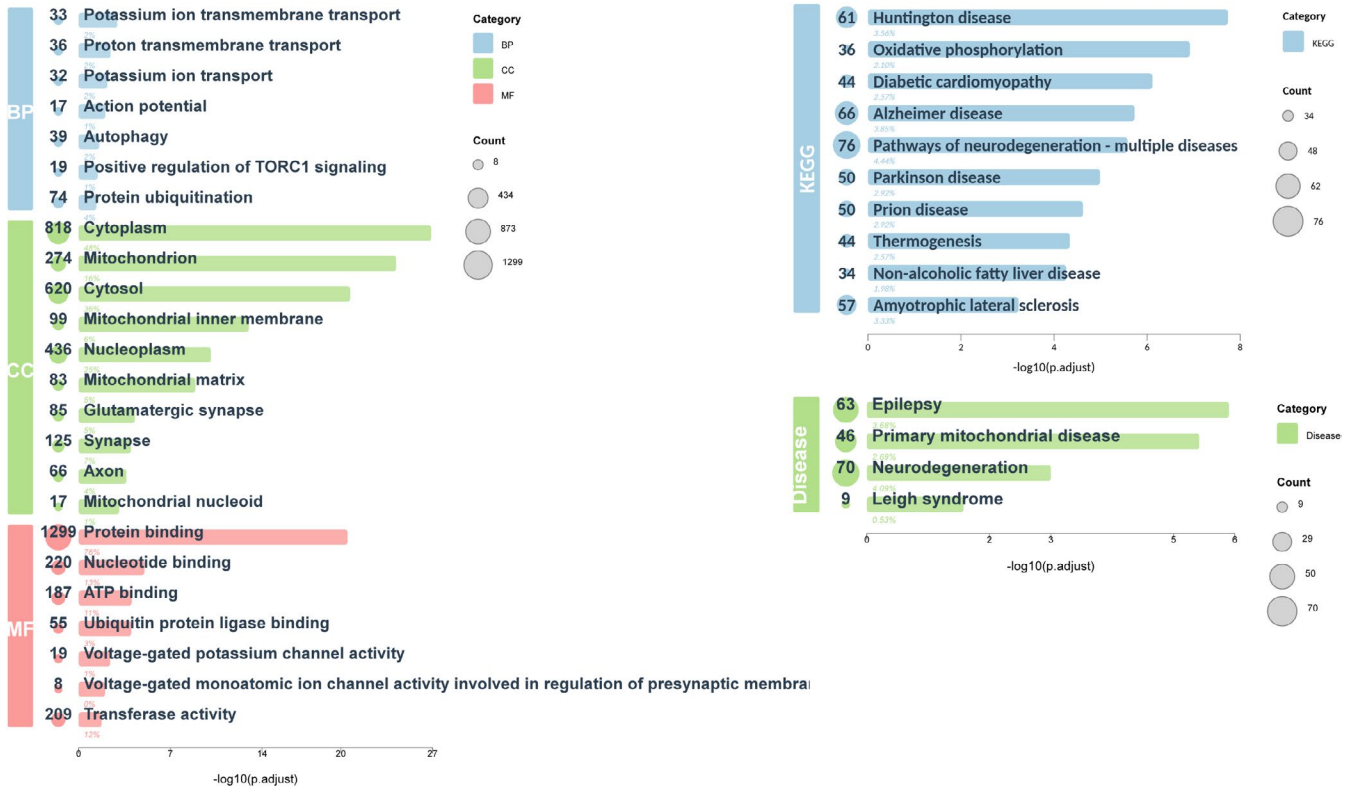

FIGURE 5 | Molecular and disease context of the adiposity-related GMV/GMD network. Gene set enrichment analyses based on genes with stable positive weights on the first partial least squares component (PLS1; bootstrap $Z > 5$), linking regional gene expression to the spatial pattern of the cross-sectional adiposity-related GMV/GMD network. All enriched genes shown here were therefore positively associated with the imaging phenotype. (A) Gene Ontology (GO) enrichment analysis showing significantly overrepresented terms across the Biological Process (BP), Cellular Component (CC), and Molecular Function (MF) domains. (B) Kyoto Encyclopedia of Genes and Genomes (KEGG) pathway enrichment analysis highlighting pathways related to mitochondrial energy metabolism, neurodegenerative disease, autophagy–lysosomal function, and metabolic regulation. (C) Disease gene set enrichment analysis showing significant overlap with neurological conditions characterized by mitochondrial dysfunction and altered neuronal excitability, including epilepsy and primary mitochondrial disorders. Only terms surviving Bonferroni correction are displayed. Bubble size (A–B) reflects the number of contributing genes, and the *x*-axis indicates enrichment significance (−log10 Bonferroni-corrected *p* values). Together, these analyses suggest that adiposity-related structural vulnerability is shaped by coordinated transcriptional programs related to neuronal energetics, synaptic signaling, and excitability regulation.

4 | Discussion

Using coordinate-based connectome mapping, we identified a reproducible large-scale network underlying adiposity-related gray matter alterations. Cross-sectional GMV/GMD reductions were concentrated in frontoparietal control, cingulo-opercular, default mode, and Visual1 systems, but this pattern varied by phenotype definition: categorical obesity preferentially involved control- and attention-related systems, whereas dimensional adiposity measures more strongly implicated default mode and association systems. In contrast, weight-loss–related GMV/GMD changes followed a distinct system-level distribution, with greater involvement of cingulo-opercular, somatomotor, and dorsal attention systems rather than a simple mirror reversal of the cross-sectional pattern. At the molecular level, the cross-sectional network was linked to coordinated transcriptional programs related to mitochondrial energetics, synaptic signaling, ion transport, and protein homeostasis.

The cross-sectional adiposity-associated network should, however, be interpreted in the context of substantial heterogeneity across the source literature. Although its split-half Dice coefficient (0.38) was significantly greater than expected under size-matched randomization, this value indicates only moderate overlap between independently derived half-sample networks. We therefore interpret this network as a reproducible core topography rather than a highly uniform spatial map, with the moderate overlap likely partly reflecting differences in adiposity phenotypes, sample characteristics, and analytic pipelines across studies. This view is further supported by the threshold-sensitivity and leave-one-out analyses, which preserved the principal network pattern despite changes in spatial extent.

Within this cross-sectional network, the frontoparietal control system showed the greatest involvement, suggesting preferential vulnerability of systems supporting executive control, goal-directed behavior, and dietary self-regulation (Lavagnino et al. 2016; Devoto et al. 2023; Gluck et al. 2017). Such a pattern may help reconcile earlier voxel-based morphometry studies that variably emphasized prefrontal and related loci by placing these heterogeneous findings within a common large-scale control-system framework. Clinically, this result is also relevant, as executive dysfunction has been associated with poorer weight-loss outcomes, and frontoparietal connectivity has been linked to improvement in eating-related cognitive control and weight loss (Devoto et al. 2023; Gluck et al. 2017; Eichen et al. 2021; Donofry et al. 2020). Beyond frontoparietal control, the next largest contributions came from the cingulo-opercular and default mode systems. Notably, Visual1 also showed substantial involvement, suggesting that adiposity-related structural alterations may extend to early sensory-attentional processing of external food cues (Pursey et al. 2014; Yang et al. 2021).

Our longitudinal findings argue against a simple mirror-reversal model of reversibility. Instead, weight-loss–related GMV/GMD changes were concentrated in cingulo-opercular, somatomotor, and dorsal attention systems, suggesting that post-weight-loss remodeling may preferentially involve salience/interoceptive processing, sensory-motor representations of eating, and attentional allocation to external food cues, rather than the higher-order association-network pattern observed cross-sectionally. The prominence of the cingulo-opercular system is consistent with prior evidence linking obesity to altered salience-network connectivity and disturbed processing of internal bodily signals and food-related salience (García-García et al. 2013). The somatomotor result is also notable, because obesity has long been linked to heightened resting activity in oral somatosensory cortex, and later neuroimaging work has continued to implicate gustatory and somatosensory processing in obesity-related eating behavior (Stice et al. 2009). For the dorsal attention system, the most plausible interpretation is altered allocation of attention to food cues, in line with evidence for food-related attentional bias in overweight and obesity (Hendrikse et al. 2015). Although longitudinal evidence remains limited, recent work further suggests that successful versus unsuccessful weight loss is accompanied by different dynamic states involving insular and motor systems, supporting the idea that post-weight-loss remodeling may preferentially affect salience-related and sensory-motor circuits.

Mechanistically, the imaging–transcriptomic findings provide a molecular complement to the system-level pattern observed in the cross-sectional network analyses (Fulcher and Fornito 2016; Dear et al. 2024). In line with the prominent involvement of higher-order association systems, functional enrichment of positively weighted PLS1 genes highlighted pathways related to mitochondrial energy metabolism, synaptic signaling, ion transport, and cellular protein homeostasis, suggesting that adiposity-related structural vulnerability is embedded in transcriptional programs supporting neuronal energetics and excitability (Godbersen et al. 2023). This interpretation is consistent with broader evidence linking obesity to systemic metabolic dysfunction, low-grade inflammation, insulin resistance, and impaired mitochondrial function (Tung et al. 2024; Hartsoe et al. 2024; Marino et al. 2025). Disease gene set enrichment further indicated overlap with neurological disorders characterized by mitochondrial dysfunction and altered neuronal excitability, including epilepsy and primary mitochondrial disorders. Although these overlaps do not imply shared disease etiology, they suggest that the cross-sectional adiposity-associated network aligns with transcriptional architectures implicated in conditions marked by energetic failure and excitability imbalance (Zhang et al. 2025; Xie et al. 2024).

4.1 | Limitations

Several limitations warrant consideration. The present connectome-based meta-analytic framework inherits constraints common to study-level coordinate-based approaches. Because the included studies reported peak coordinates rather than unthresholded whole-brain statistical maps, individual contrasts could not be weighted by effect size or sample size, and residual heterogeneity related to sample composition, adiposity phenotypes, imaging protocols, preprocessing pipelines, and analytic strategies could not be explicitly regressed out or fully modeled. As a result, individual contrasts contribute equally at the coordinate level within the current reconstruction framework, regardless of study size. The resulting vulnerability networks should therefore be interpreted cautiously as probabilistic maps of cross-study spatial convergence rather than as precise quantitative estimates of regional effect magnitude. This limitation is particularly relevant when interpreting the relative prominence of specific network components, which may partly reflect between-study differences that could not be explicitly modeled in the present design. In addition, both the normative functional connectome and gene expression data were derived from independent healthy samples, which further limits causal inference at the individual level and precludes direct testing of subject-specific relationships between adiposity, brain structure, and gene expression. Imaging–transcriptomic analyses were additionally restricted to left-hemisphere regions because of the spatial sampling characteristics of the Allen Human Brain Atlas, which may constrain the generalizability of these transcriptomic inferences across the full spatial distribution of the imaging phenotype. Longitudinal weight-loss analyses provide useful insight into structural plasticity, but follow-up durations were relatively short and heterogeneous, which limits conclusions about long-term reversibility. Future studies combining longitudinal neuroimaging, detailed metabolic phenotyping, and genetic data will be important for refining these inferences.

5 | Conclusions

In summary, we reconciled heterogeneous adiposity-related gray matter findings within a coordinate-based connectome mapping framework and showed that they converge on a reproducible large-scale network. This network was most prominently expressed in frontoparietal control, cingulo-opercular, default mode, and Visual1 systems, while categorical obesity and dimensional adiposity measures showed partially dissociable system-level patterns. GMV/GMD increases following weight loss exhibited a distinct distribution, with greater involvement of cingulo-opercular, somatomotor, and dorsal attention systems, arguing against a simple mirror reversal of the cross-sectional network. Imaging transcriptomic analyses further linked the cross-sectional network to coordinated molecular programs related to mitochondrial energetics, synaptic signaling, ion transport, and protein homeostasis. These findings may help inform the identification of network-level targets for monitoring and potentially guiding interventions aimed at mitigating adiposity-related brain vulnerability. Together, these findings advance the network-level characterization of adiposity-related brain structural vulnerability and suggest that post-weight-loss remodeling engages partly distinct functional systems.

Author Contributions

Y.L. and W.Z. conceived and designed the study. Y.L. and M.L. performed the literature search and study selection. Y.L. and G.Z. extracted data and conducted the quantitative synthesis and connectome mapping. H.Z. performed the imaging transcriptomic analyses. Y.L. drafted the manuscript. All authors critically revised the manuscript for important intellectual content and approved the final version.

Acknowledgments

We thank all participants for their contribution, and we acknowledge the developers of the open neuroimaging resources and toolboxes used in this study.

Funding

This study was supported by the Provincial Science and Technology Innovation Strategy Special Project Funding Program (No. STKJ2023042) and the Natural Science Foundation of Guangdong Province (2024A1515011698).

Ethics Statement

This study is a coordinate-based meta-analysis of previously published human neuroimaging studies and publicly available reference datasets. It did not involve new participant recruitment, enrollment, or primary data collection. Therefore, the Human Brain Mapping Participant Inclusivity requirement is not applicable to this work.

Conflicts of Interest

The authors declare no conflicts of interest.

Data Availability Statement

The data that support the findings of this study are openly available in Open Science Framework (OSF) at https://doi.org/10.17605/OSF.IO/SPJZD.

References

An, K., D. Zhang, M. Gao, et al. 2026. "Parsing Neurobiological Heterogeneity in Treatment-Resistant Depression Using Brain Network Localization." *Neurobiology of Disease* 222: 107363.

Arnatkeviciute, A., R. D. Markello, B. D. Fulcher, B. Misic, and A. Fornito. 2023. "Toward Best Practices for Imaging Transcriptomics of the Human Brain." *Biological Psychiatry* 93, no. 5: 391–404.

Arnold, S. E., Z. Arvanitakis, S. L. Macauley-Rambach, et al. 2018. "Brain Insulin Resistance in Type 2 Diabetes and Alzheimer Disease: Concepts and Conundrums." *Nature Reviews Neurology* 14, no. 3: 168–181.

Brooks, S. J., C. Benedict, J. Burgos, et al. 2013. "Late-Life Obesity Is Associated With Smaller Global and Regional Gray Matter Volumes: A Voxel-Based Morphometric Study." *International Journal of Obesity (London, England: 2005)* 37, no. 2: 230–236.

Buckner, R. L., J. R. Andrews-Hanna, and D. L. Schacter. 2008. "The Brain's Default Network." *Annals of the New York Academy of Sciences* 1124, no. 1: 1–38.

Cheng, Y., H. Cai, S. Liu, et al. 2025. "Brain Network Localization of Gray Matter Atrophy and Neurocognitive and Social Cognitive Dysfunction in Schizophrenia." *Biological Psychiatry* 97, no. 2: 148–156.

Crossley, N. A., A. Mechelli, J. Scott, et al. 2014. "The Hubs of the Human Connectome Are Generally Implicated in the Anatomy of Brain Disorders." *Brain* 137, no. 8: 2382–2395.

Dear, R., K. Wagstyl, J. Seidlitz, et al. 2024. "Cortical Gene Expression Architecture Links Healthy Neurodevelopment to the Imaging, Transcriptomics and Genetics of Autism and Schizophrenia." *Nature Neuroscience* 27, no. 6: 1075–1086.

Devoto, F., A. Ferrulli, G. Banfi, et al. 2023. "How Images of Food Become Cravingly Salient in Obesity." *Obesity (Silver Spring)* 31, no. 9: 2294–2303.

Donofry, S. D., C. M. Stillman, and K. I. Erickson. 2020. "A Review of the Relationship Between Eating Behavior, Obesity and Functional Brain Network Organization." *Social Cognitive and Affective Neuroscience* 15, no. 10: 1157–1181.

Eichen, D. M., E. K. Pasquale, E. W. Twamley, and K. N. Boutelle. 2021. "Targeting Executive Function for Weight Loss in Adults With Overweight or Obesity." *Physiology & Behavior* 240: 113540.

Fan, L., H. Li, J. Zhuo, et al. 2016. "The Human Brainnetome Atlas: A New Brain Atlas Based on Connectional Architecture." *Cerebral Cortex* 26, no. 8: 3508–3526.

Fang, L., Y. Zhuang, M. Zhang, et al. 2026. "Dietary and Metabolic Reprogramming Alleviates Neurodegeneration: A Review of Mechanisms and Clinical Implications." *Frontiers in Nutrition* 13: 1706597.

Figley, C. R., J. S. Asem, E. L. Levenbaum, J. S. A. Asem, and S. M. Courtney. 2016. "Effects of Body Mass Index and Body Fat Percent on Default Mode, Executive Control, and Salience Network Structure and Function." *Frontiers in Neuroscience* 10: 234.

Fornito, A., A. Zalesky, and M. Breakspear. 2015. "The Connectomics of Brain Disorders." *Nature Reviews Neuroscience* 16, no. 3: 159–172.

Fox, M. D. 2018. "Mapping Symptoms to Brain Networks With the Human Connectome." *New England Journal of Medicine* 379, no. 23: 2237–2245.

Fulcher, B. D., and A. Fornito. 2016. "A Transcriptional Signature of Hub Connectivity in the Mouse Connectome." *Proceedings of the National Academy of Sciences* 113, no. 5: 1435–1440.

García-García, I., M. Á. Jurado, M. Garolera, et al. 2013. "Alterations of the Salience Network in Obesity: A Resting-State fMRI Study." *Human Brain Mapping* 34, no. 11: 2786–2797.

García-García, I., A. Michaud, M. Dadar, et al. 2019. "Neuroanatomical Differences in Obesity: Meta-Analytic Findings and Their Validation in an Independent Dataset." *International Journal of Obesity* 43, no. 5: 943–951.

Gluck, M. E., P. Viswanath, and E. J. Stinson. 2017. "Obesity, Appetite, and the Prefrontal Cortex." *Current Obesity Reports* 6, no. 4: 380–388.

Godbersen, G. M., S. Klug, W. Wadsak, et al. 2023. "Task-Evoked Metabolic Demands of the Posteromedial Default Mode Network Are Shaped by Dorsal Attention and Frontoparietal Control Networks." *eLife* 12: e84683.

Hartsoe, P., F. Holguin, and H. W. Chu. 2024. "Mitochondrial Dysfunction and Metabolic Reprogramming in Obesity and Asthma." *International Journal of Molecular Sciences* 25, no. 5: 2944.

Hayakawa, Y. K., H. Sasaki, H. Takao, et al. 2018. "The Relationship of Waist Circumference and Body Mass Index to Grey Matter Volume in Community Dwelling Adults With Mild Obesity." *Obesity Science & Practice* 4, no. 1: 97–105.

He, Q., C. Chen, Q. Dong, G. Xue, Z. L. Lu, and A. Bechara. 2015. "Gray and White Matter Structures in the Midcingulate Cortex Region Contribute to Body Mass Index in Chinese Young Adults." *Brain Structure & Function* 220, no. 1: 319–329.

Hendrikse, J. J., R. L. Cachia, E. J. Kothe, S. McPhie, H. Skouteris, and M. J. Hayden. 2015. "Attentional Biases for Food Cues in Overweight and Individuals With Obesity: A Systematic Review of the Literature." *Obesity Reviews* 16, no. 5: 424–432.

Hidese, S., M. Ota, J. Matsuo, et al. 2022. "Association of Body Mass Index and Its Classifications With Gray Matter Volume in Individuals With a Wide Range of Body Mass Index Group: A Whole-Brain Magnetic Resonance Imaging Study." *Frontiers in Human Neuroscience* 16: 926804.

Holmes, A. J., M. O. Hollinshead, T. M. O'keefe, et al. 2015. "Brain Genomics Superstruct Project Initial Data Release With Structural, Functional, and Behavioral Measures." *Scientific Data* 2: 150031.

Honea, R. A., A. N. Szabo-Reed, R. J. Lepping, et al. 2016. "Voxel-Based Morphometry Reveals Brain Gray Matter Volume Changes in Successful Dieters." *Obesity (Silver Spring)* 24, no. 9: 1842–1848.

Horstmann, A., F. P. Busse, D. Mathar, et al. 2011. "Obesity-Related Differences Between Women and Men in Brain Structure and Goal-Directed Behavior." *Frontiers in Human Neuroscience* 5: 58.

Huang, Y., X. Li, T. Jackson, et al. 2019. "Interaction Effect of Sex and Body Mass Index on Gray Matter Volume." *Frontiers in Human Neuroscience* 13: 360.

Janowitz, D., K. Wittfeld, J. Terock, et al. 2015. "Association Between Waist Circumference and Gray Matter Volume in 2344 Individuals From Two Adult Community-Based Samples." *NeuroImage* 122: 149–157.

Jauch-Chara, K., F. Binkofski, M. Loebig, et al. 2015. "Blunted Brain Energy Consumption Relates to Insula Atrophy and Impaired Glucose Tolerance in Obesity." *Diabetes* 64, no. 6: 2082–2091.

Ji, J. L., M. spronk, K. Kulkarni, G. Repovš, A. Anticevic, and M. W. Cole. 2019. "Mapping the Human Brain's Cortical-Subcortical Functional Network Organization." *NeuroImage* 185: 35–57.

Karlsson, H. K., J. J. Tuulari, J. Hirvonen, et al. 2013. "Obesity Is Associated With White Matter Atrophy: A Combined Diffusion Tensor Imaging and Voxel-Based Morphometric Study." *Obesity (Silver Spring)* 21, no. 12: 2530–2537.

Kennedy, J. T., P. F. Collins, and M. Luciana. 2016. "Higher Adolescent Body Mass Index Is Associated With Lower Regional Gray and White Matter Volumes and Lower Levels of Positive Emotionality." *Frontiers in Neuroscience* 10: 413.

Kharabian Masouleh, S., K. Arélin, A. Horstmann, et al. 2016. "Higher Body Mass Index in Older Adults Is Associated With Lower Gray Matter Volume: Implications for Memory Performance." *Neurobiology of Aging* 40: 1–10.

Kullmann, S., M. Heni, M. Hallschmid, A. Fritsche, H. Preissl, and H. U. Häring. 2016. "Brain Insulin Resistance at the Crossroads of Metabolic and Cognitive Disorders in Humans." *Physiological Reviews* 96, no. 4: 1169–1209.

Kurth, F., J. G. Levitt, O. R. Phillips, et al. 2013. "Relationships Between Gray Matter, Body Mass Index, and Waist Circumference in Healthy Adults." *Human Brain Mapping* 34, no. 7: 1737–1746.

Lavagnino, L., D. Arnone, B. Cao, et al. 2016. "Inhibitory Control in Obesity and Binge Eating Disorder: A Systematic Review and Meta-Analysis of Neurocognitive and Neuroimaging Studies." *Neuroscience & Biobehavioral Reviews* 68: 714–726.

Lefort-Besnard, J., T. E. Nichols, and C. Maumet. 2025. "Statistical Inference for Same Data Meta-Analysis in Neuroimaging Multiverse Analyzes." *Imaging Neuroscience* 3: 00513.

Li, G., Y. Hu, W. Zhang, et al. 2023. "Brain Functional and Structural Magnetic Resonance Imaging of Obesity and Weight Loss Interventions." *Molecular Psychiatry* 28, no. 4: 1466–1479.

Li, L., H. Yu, M. Zhong, et al. 2022. "Gray Matter Volume Alterations in Subjects With Overweight and Obesity: Evidence From a Voxel-Based Meta-Analysis." *Frontiers in Psychiatry* 13: 955741.

Liu, C., Y. Song, X. Zhao, et al. 2026. "Brain Network Localization of Anhedonia." *Translational Psychiatry* 16, no. 1: 214.

Liu, W., N. Li, D. Tang, L. Qin, and Z. Zhu. 2025. "Multimodal Neuroimaging of Obesity: From Structural-Functional Mechanisms to Precision Interventions." *Brain Sciences* 15, no. 5: 446.

Livingston, G., J. Huntley, K. Y. Liu, et al. 2024. "Dementia Prevention, Intervention, and Care: 2024 Report of the Lancet Standing Commission." *Lancet* 404, no. 10452: 572–628.

Ma, H., H. Liu, W. Zhang, et al. 2026. "Network Localization of Brain Functional Effects of Ketamine Treatment for Major Depression." *European Psychiatry* 69, no. 1: e28.

Marino, F., L. Petrella, F. Cimmino, et al. 2025. "From Obesity to Mitochondrial Dysfunction in Peripheral Tissues and in the Central Nervous System." *Biomolecules* 15, no. 5: 638.

Mathar, D., A. Horstmann, B. Pleger, A. Villringer, and J. Neumann. 2016. "Is It Worth the Effort? Novel Insights Into Obesity-Associated Alterations in Cost-Benefit Decision-Making." *Frontiers in Behavioral Neuroscience* 9: 360.

Maynard, R. D. 2025. "A Defining Moment: A Consensus on the Diagnostic Criteria for Clinical Obesity." *Clinical Chemistry* 71, no. 9: 1009–1010.

Michaud, A., M. Dadar, M. Pelletier, et al. 2020. "Neuroanatomical Changes in White and Grey Matter After Sleeve Gastrectomy." *NeuroImage* 213: 116696.

Miller, A. A., and S. J. Spencer. 2014. "Obesity and Neuroinflammation: A Pathway to Cognitive Impairment." *Brain, Behavior, and Immunity* 42: 10–21.

Morys, F., C. Tremblay, S. Rahayel, et al. 2024. "Neural Correlates of Obesity Across the Lifespan." *Communications Biology* 7, no. 1: 656.

Nouwen, A., A. Chambers, M. Chechlacz, et al. 2017. "Microstructural Abnormalities in White and Gray Matter in Obese Adolescents With and Without Type 2 Diabetes." *NeuroImage: Clinical* 16: 43–51.

O'brien, P. D., L. M. Hinder, B. C. Callaghan, and E. L. Feldman. 2017. "Neurological Consequences of Obesity." *Lancet Neurology* 16, no. 6: 465–477.

Opel, N., R. Redlich, C. Kaehler, et al. 2017. "Prefrontal Gray Matter Volume Mediates Genetic Risks for Obesity." *Molecular Psychiatry* 22, no. 5: 703–710.

Pannacciulli, N., A. Del Parigi, K. Chen, et al. 2006. "Brain Abnormalities in Human Obesity: A Voxel-Based Morphometric Study." *NeuroImage* 31, no. 4: 1419–1425.

Peraza, J. A., J. D. Kent, R. W. Blair, et al. 2025. "Advancing Image-Based Meta-Analysis Through Systematic Use of Crowdsourced NeuroVault Data." *Scientific Reports* 15, no. 1: 36582.

Prehn, K., R. Jumpertz Von Schwartzenberg, K. Mai, et al. 2017. "Caloric Restriction in Older Adults-Differential Effects of Weight Loss and Reduced Weight on Brain Structure and Function." *Cerebral Cortex* 27, no. 3: 1765–1778.

Prehn, K., T. Profitlich, I. Rangus, et al. 2020. "Bariatric Surgery and Brain Health-A Longitudinal Observational Study Investigating the Effect of Surgery on Cognitive Function and Gray Matter Volume." *Nutrients* 12, no. 1: 127.

Pursey, K. M., P. Stanwell, R. J. Callister, K. Brain, C. E. Collins, and T. L. Burrows. 2014. "Neural Responses to Visual Food Cues According to Weight Status: A Systematic Review of Functional Magnetic Resonance Imaging Studies." *Frontiers in Nutrition* 1: 7.

Qu, Y., H.-Y. Hu, Y.-N. Ou, et al. 2020. "Association of Body Mass Index With Risk of Cognitive Impairment and Dementia: A Systematic Review and Meta-Analysis of Prospective Studies." *Neuroscience & Biobehavioral Reviews* 115: 189–198.

Rubino, F., D. E. Cummings, R. H. Eckel, et al. 2025. "Definition and Diagnostic Criteria of Clinical Obesity." *Lancet Diabetes and Endocrinology* 13, no. 3: 221–262.

Rullmann, M., S. Preusser, S. Poppitz, et al. 2018. "Gastric-Bypass Surgery Induced Widespread Neural Plasticity of the Obese Human Brain." *NeuroImage* 172: 853–863.

Rullmann, M., S. Preusser, S. Poppitz, et al. 2019. "Adiposity Related Brain Plasticity Induced by Bariatric Surgery." *Frontiers in Human Neuroscience* 13: 290.

Shan, H., P. Li, H. Liu, et al. 2019. "Gray Matter Reduction Related to Decreased Serum Creatinine and Increased Triglyceride, Hemoglobin A1C, and Low-Density Lipoprotein in Subjects With Obesity." *Neuroradiology* 61, no. 6: 703–710.

She, M., Y. Sun, Z. Yan, et al. 2026. "Network Localization of Brain Structural and Functional Abnormalities in Association With Rumination." *NeuroImage* 333: 121929.

Shott, M. E., M. A. Cornier, V. A. Mittal, et al. 2015. "Orbitofrontal Cortex Volume and Brain Reward Response in Obesity." *International Journal of Obesity (London)* 39, no. 2: 214–221.

Smucny, J., M. A. Cornier, L. C. Eichman, E. A. Thomas, J. L. Bechtell, and J. R. Tregellas. 2012. "Brain Structure Predicts Risk for Obesity." *Appetite* 59, no. 3: 859–865.

Steele, N., A. A. Huggins, R. A. Morey, et al. 2025. "Image-Based Meta- and Mega-Analysis (IBMMA): A Unified Framework for Large-Scale, Multi-Site, Neuroimaging Data Analysis." *NeuroImage* 322: 121554.

Stice, E., S. Spoor, J. Ng, and D. H. Zald. 2009. "Relation of Obesity to Consummatory and Anticipatory Food Reward." *Physiology & Behavior* 97: 551–560.

Stubbs, J. L., J. J. Taylor, S. H. Siddiqi, et al. 2023. "Heterogeneous Neuroimaging Findings Across Substance Use Disorders Localize to a Common Brain Network." *Nature Mental Health* 1, no. 10: 772–781.

Taki, Y., S. Kinomura, K. Sato, et al. 2008. "Relationship Between Body Mass Index and Gray Matter Volume in 1,428 Healthy Individuals." *Obesity (Silver Spring)* 16, no. 1: 119–124.

Tang, X., W. Zhao, M. Lu, et al. 2021. "Relationship Between Central Obesity and the Incidence of Cognitive Impairment and Dementia From Cohort Studies Involving 5,060,687 Participants." *Neuroscience & Biobehavioral Reviews* 130: 301–313.

The Lancet Diabetes Endocrinology. 2025. "Redefining Obesity: Advancing Care for Better Lives." *Lancet Diabetes and Endocrinology* 13, no. 2: 75.

Tung, P. W., V. V. Thaker, D. Gallagher, and A. Kupsco. 2024. "Mitochondrial Health Markers and Obesity-Related Health in Human Population Studies: A Narrative Review of Recent Literature." *Current Obesity Reports* 13, no. 4: 724–738.

Tuulari, J. J., H. K. Karlsson, O. Antikainen, et al. 2016. "Bariatric Surgery Induces White and Grey Matter Density Recovery in the Morbidly Obese: A Voxel-Based Morphometric Study." *Human Brain Mapping* 37, no. 11: 3745–3756.

Vaishnavi, S. N., A. G. Vlassenko, M. M. Rundle, A. Z. Snyder, M. A. Mintun, and M. E. Raichle. 2010. "Regional Aerobic Glycolysis in the Human Brain." *Proceedings of the National Academy of Sciences of the United States of America* 107, no. 41: 17757–17762.

Walther, K., A. C. Birdsill, E. L. Glisky, and L. Ryan. 2010. "Structural Brain Differences and Cognitive Functioning Related to Body Mass Index in Older Females." *Human Brain Mapping* 31, no. 7: 1052–1064.

Wang, H., B. Wen, J. Cheng, and H. Li. 2017. "Brain Structural Differences Between Normal and Obese Adults and Their Links With Lack of Perseverance, Negative Urgency, and Sensation Seeking." *Scientific Reports* 7: 40595.

Wang, Y., G. Ji, Y. Hu, et al. 2020. "Laparoscopic Sleeve Gastrectomy Induces Sustained Changes in Gray and White Matter Brain Volumes and Resting Functional Connectivity in Obese Patients." *Surgery for Obesity and Related Diseases* 16, no. 1: 1–9.

Weise, C. M., T. Bachmann, and B. Pleger. 2019. "Brain Structural Differences in Monozygotic Twins Discordant for Body Mass Index." *NeuroImage* 201: 116006.

Weise, C. M., P. Piaggi, M. Reinhardt, et al. 2017. "The Obese Brain as a Heritable Phenotype: A Combined Morphometry and Twin Study." *International Journal of Obesity (London, England: 2005)* 41, no. 3: 458–466.

Weise, C. M., P. Thiyyagura, E. M. Reiman, K. Chen, and J. Krakoff. 2013. "Fat-Free Body Mass but Not Fat Mass Is Associated With Reduced Gray Matter Volume of Cortical Brain Regions Implicated in Autonomic and Homeostatic Regulation." *NeuroImage* 64: 712–721.

Xie, W., S. Koppula, M. B. Kale, et al. 2024. "Unraveling the Nexus of Age, Epilepsy, and Mitochondria: Exploring the Dynamics of Cellular Energy and Excitability." *Frontiers in Pharmacology* 15: 1469053.

Yang, Y., Q. Wu, and F. Morys. 2021. "Brain Responses to High-Calorie Visual Food Cues in Individuals With Normal-Weight or Obesity: An Activation Likelihood Estimation Meta-Analysis." *Brain Sciences* 11, no. 12: 1587.

Yao, L., W. Li, Z. Dai, and C. Dong. 2016. "Eating Behavior Associated With Gray Matter Volume Alternations: A Voxel Based Morphometry Study." *Appetite* 96: 572–579.

Yokum, S., J. Ng, and E. Stice. 2012. "Relation of Regional Gray and White Matter Volumes to Current BMI and Future Increases in BMI: A Prospective MRI Study." *International Journal of Obesity (London, England: 2005)* 36, no. 5: 656–664.

Zhang, X., Z. Wu, X. Zhou, and H. Tao. 2025. "Mitochondrial Dysfunction in Epilepsy: Mechanistic Insights and Clinical Strategies." *Molecular Biology Reports* 52, no. 1: 470.

Zhang, Y., G. Ji, M. Xu, et al. 2016. "Recovery of Brain Structural Abnormalities in Morbidly Obese Patients After Bariatric Surgery." *International Journal of Obesity (London, England: 2005)* 40, no. 10: 1558–1565.

Zhou, H., Y. Hu, G. Li, et al. 2025. "Obesity Is Associated With Progressive Brain Structural Changes." *Obesity (Silver Spring)* 33, no. 4: 709–719.

Supporting Information

Additional supporting information can be found online in the Supporting Information section. **Data S1:** PLS gene weights and bootstrap Z scores (Excel file). **Data S2:** Functional enrichment results (GO, KEGG, and disease gene sets) exported from DAVID (Excel file). **Table S1:** Characteristics of included structural MRI studies and eligible contrasts. **Table S2:** Quality and methodological characteristics of included studies. **Table S3:** System-level distribution and within-network vulnerability of abnormal voxels within the CAB-NP atlas mask across the 12 large-scale CAB-NP networks. **Figure S1:** PRISMA flow diagram of study selection. Flow diagram illustrating the identification, screening, eligibility assessment, and inclusion of studies in the coordinate-based meta-analysis of obesity-related gray matter alterations. Records were identified through systematic database searches, duplicates were removed, and full-text articles were assessed according to predefined inclusion and exclusion criteria. Only whole-brain structural MRI studies reporting stereotactic coordinates of gray matter volume or density alterations in adolescent or adult samples were included in the quantitative synthesis. **Figure S2:** Sensitivity analyses across alternative convergence thresholds. Network maps of the obesity-related network are shown at convergence thresholds of ≥ 0.45, ≥ 0.50 (primary analysis), and ≥ 0.55. Lowering the threshold resulted in spatial expansion of the network, whereas more stringent thresholding led to progressively sparser maps, while preserving the core spatial pattern. Thresholds above this range (e.g., ≥ 0.60) yielded minimal surviving voxels and were therefore not visualized. **Figure S3:** Associations of significant PLS components with the imaging phenotype. (A) Scatter plot showing the association between PLS1 scores and the imaging phenotype across left-hemisphere regions ($r = 0.633$, $p = 0.011$). (B) Scatter plot showing the association between PLS2 scores and the imaging phenotype across left-hemisphere regions ($r = 0.584$, $p = 0.006$). Both components reached significance by spatial permutation testing, but downstream enrichment analyses were restricted to positively weighted PLS1 genes because PLS1 represented the dominant latent variable.